Check for updates

Research Article

NANOMATERIALS AND NANOTECHNOLOGY

Nanomaterials and Nanotechnology
Volume 12: 1–6
© The Author(s) 2022
Article reuse guidelines:
sagepub.com/journals-permissions
DOI: 10.1177/18479804221085790
journals.sagepub.com/home/nax
SAGE

Optically controlled dual-band quantum dot infrared photodetector

Stefano Vichi[1], Sergio Bietti[2], Francesco Basso Basset[3], Artur Tuktamyshev[1], Alexey Fedorov[4] and Stefano Sanguinetti[2]

Abstract

We present the design for a novel type of dual-band photodetector in the thermal infrared spectral range, the Optically Controlled Dual-band quantum dot Infrared Photodetector (OCDIP). This concept is based on a quantum dot ensemble with a unimodal size distribution, whose absorption spectrum can be controlled by optically injected carriers. An external pumping laser varies the electron density in the QDs, permitting to control the available electronic transitions and thus the absorption spectrum. We grew a test sample which we studied by AFM and photoluminescence. Based on the experimental data, we simulated the infrared absorption spectrum of the sample, which showed two absorption bands at 5.85 μm and 8.98 μm depending on the excitation power.

Keywords

Infrared photodetector, quantum dot, droplet epitaxy

Topic Area: Nanooptics and Nanophotonics
Topic Editor: Nezih Pala
Associate Editor: Andres Cantarero

Introduction

Thermal infrared (TIR) remote sensing plays a key role in different fields, which span military, commercial, public, and academic domains and it is of particular interest in Earth science research, where it permits the modeling of surface thermal energy.[1] TIR remote sensing is based on the detection of objects infrared emission at multiple wavelengths in order to eliminate spurious effects and reconstruct the real object temperature. These wavelengths, which are typically located between 8 and 13 μm, are chosen in the spectral region with the highest atmospheric transmissivity. A two-channel (or split-window) algorithm requires at least two absorption bands in the TIR region[2,3] in order to determine the absolute temperature of the studied surface. This wavelength restriction can be avoided if the distance from the radiation source is sufficiently low to make the atmospheric absorption negligible. This opens up the possibility to detect temperatures in the 200–300°C range, which corresponds to an emission peak of approximately 5.5 μm. Measuring multiple wavelengths typically requires different detectors with separate cooling systems and electronics. However, the difficulties and costs of assembling several detectors can be overcome by using a single detector responding in multiple bands. For this reason, dual-band quantum well infrared photodetectors (QWIPs) have been extensively researched and significant progress has been made in the past years.[4] In recent times, quantum dots (QDs) infrared photodetectors (QDIPs)[5–7] have emerged as a promising alternative to QWIPs. Compared to these, QDIPs offer numerous advantages,

[1]INFN, Sezione di Milano-Bicocca, Milano, Italy
[2]L-NESS and Department of Materials Science, University of Milano-Bicocca, Milano, Italy
[3]Department of Physics, Sapienza University of Rome, Rome, Italy
[4]L-NESS and CNR-IFN, Como, Italy

Corresponding author:
Stefano Vichi, INFN, Sezione di Milano-Bicocca, via R.Cozzi 55, Milano I-20126, Italy.
Email: stefano.vichi@unimib.it

Creative Commons CC BY: This article is distributed under the terms of the Creative Commons Attribution 4.0 License (https://creativecommons.org/licenses/by/4.0/) which permits any use, reproduction and distribution of the work without further permission provided the original work is attributed as specified on the SAGE and Open Access pages (https://us.sagepub.com/en-us/nam/open-access-at-sage).

including sensitivity to normally incident light, low leakage current, and low dark current.[8] In order to detect multiple wavelengths, most of the reported multicolor QDIPs incorporate QDs with different sizes.[5,9] Due to the three-dimensional quantum size effect, the TIR detection bands can be tuned in the 5–12 μm range. In state-of-the-art dual-band QDIP, two QD ensembles with different sizes are present and thus different detection bands can be selected. Here we present the idea for a novel type of dual-band photodetector in the TIR spectral window, the Optically Controlled Dual-band Infrared Photodetector (OCDIP), which avoids the disadvantages of having multiple QDs ensembles and at the same time allows the dynamical tuning of the optical response for band contribution separation. The OCDIP design is based on a single QD ensemble whose absorption spectrum can be controlled by optically injected carriers. An external pumping laser varies the electron density in the QDs, permitting to control the available electronic transitions and thus the absorption spectrum. This idea is derived from the working principle of the intermediate band solar cells, in which the absorption can be controlled by a two-photon process.[10,11] In the OCDIP however the pumping laser is used to selectively fill the QDs ground and excited state in order to obtain one or two distinguishable absorption bands. In order to be achievable, it is fundamental to engineer the QD states in order to have a clear separation between the ground state and the first excited state. In this work we also propose a geometry of the nanostructures in order to obtain two absorption bands at 5.85 μm and 8.98 μm. The proposed structure would be particularly suitable for the detection of forest fires, since the wood ignition temperature of approximately 250° C corresponds to an IR emission peak of 5.5 μm.

OCDIP concept

In order to fill the QDs ground state, usually a δ-doping layer is grown in the proximity of the QDs layers.[12] Electrons are thermally excited from donor states into QDs, populating them and contributing to the absorption process. However, since the doping density is fixed from the growth conditions, it is not possible to dynamically control the electron density inside QDs and thus the absorption spectrum. Furthermore, there are several problems related to the δ-doping layer, such as potential fluctuations, random distribution of dopants, leakage current paths,[13] internal electric field[14] and increase in dark current.[15] Our approach to fill QDs ground state is designed to enable the dynamical control of the QDs electron population. In the OCDIP approach, electron-hole pairs are generated in the barrier due to optical excitation and then are captured by QDs. The electron density inside QDs is proportional to the optical pumping power and therefore a change of the incident power affects QDs electron population.

Usually more than two confined states are present in QDs; if only the QD ground state is populated, a single intraband absorption peak is present, corresponding to the difference in energy between the electron ground state and the continuum. A second absorption band, originating from the transition of electrons confined in the first excited state, can be accessed by increasing the carrier population inside the QDs enough to saturate its ground state. After that, the first excited state starts to fill, enabling also the transition from the first excited state to the continuum. The control over QDs electron population, on which is based the OCDIP idea, is thus the key to selectively obtain one or two absorption bands and dynamically switch between them. Höglund et al. demonstrated that resonant optical pumping across bandgap can be used to artificially dope QDs and selectively obtain dual-band absorption in a dots-in-a-well infrared photodetector (DWELL).[16] However, this system relies on resonant excitation and therefore needs two high-power lasers of different wavelengths to pump electrons in the ground and first exited states of the QDs respectively. Due to the low absorption of the resonant excitation, this is not a particularly efficient system to dynamically control the electron population in the QDs. These difficulties can be overcome by combining the idea of Höglund with the one of Ramiro,[17] who recently showed an optically triggered single-band IR photodetector. In such a design the absorption of the TIR band is triggered by an external light source which injects carriers in the QDs. Their idea of filling the ground state by optical injection can be further extended to obtain dynamical control of QDs electron density, in order to achieve the dual-band photoresponse described in this paper.

Experimental

In order to demonstrate the feasibility of this concept, we grew GaAs QDs in an Al0.3Ga0.7As barrier by droplet epitaxy.[18,19] We chose this technique over the more common Stranski-Krastanov since it is the one that allows the best control over the nucleation process and to achieve very low size dispersion[20,21] which leads to a narrow absorption line.[22]

The sample was prepared in a conventional III-V molecular beam epitaxy machine equipped with cracked valved As cell and in-situ reflection high energy electron diffraction. The samples were grown on a GaAs (001) 2” substrate. After the deposition of a buffer layer of GaAs with a thickness of 500 nm an Al0.3Ga0.7As layer of 150 nm thickness acting as a potential barrier for the QDs, Ga droplets were formed by irradiating the surface with a flux of 0.02 ML/s at a temperature of 300°C. The first monolayer of Ga reacts with the As-rich c(4x4) reconstructed surface establishing a Ga-stabilized (4 x 6) reconstruction. The droplets are then formed by the remaining Ga coverage, resulting in the deposition of 0.06 MLs. During the droplet formation step it is possible to control the density and volume of the droplets by controlling substrate temperature and deposited Ga

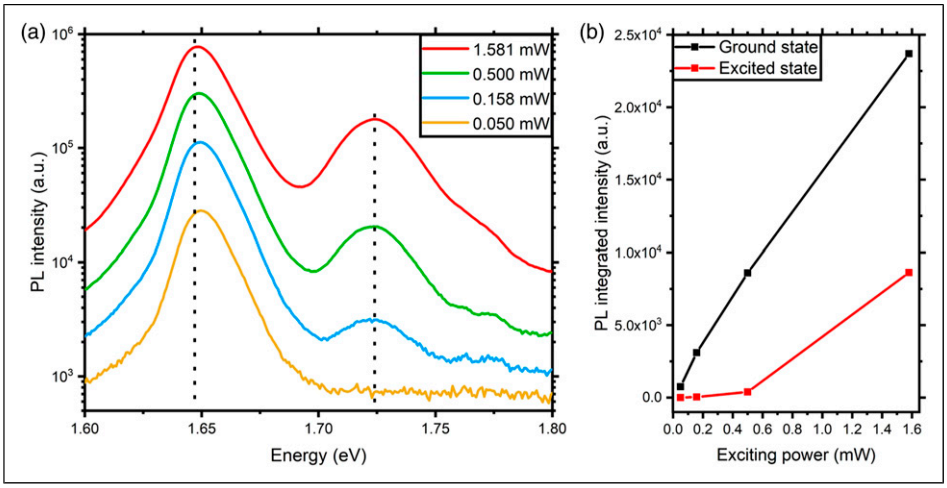

Figure 1. (a) Photoluminescence spectrum as a function of incident power measured at 90 K. The dashed lines indicate the simulated transition energies of the ground state transition (1.647 eV) and of the first excited state transition (1.724 eV). (b) Photoluminescence integrated intensity of the ground and first excited states transitions as a function of the incident power.

amount. More in details, the droplet density is affected by substrate temperature and Ga flux, while the droplet volume is mostly affected by the Ga amount.[18,23] Then the Ga droplets were exposed to an As beam equivalent pressure of 5.10–5 torr at 150°C for 3 min to crystallize into GaAs. During the crystallization step, the size and morphology of the QDs can be controlled by changing substrate temperature and As pressure.[18] Subsequently, the nanocrystals underwent a flash procedure, consisting of a 10 min heating at 380°C in an As pressure of 4×10^{-6} torr in order to improve the crystal quality of the dots and of the AlGaAs layer grown at low temperature on top of the QDs.[24] Finally, the QDs were covered with another layer of 10 nm of Al0.3Ga0.7As deposited at low temperature followed by 140 nm at 580°C, and capped with 10 nm of GaAs. After the growth, the sample underwent a rapid thermal annealing in nitrogen atmosphere at 750°C for 4 min to improve the quality of the barrier layer and of the QDs.[25]

Photoluminescence measurements (PL) were performed at different temperatures and powers in order to study the filling of QDs. During photoluminescence (PL) measurements the sample was kept in a closed-cycle cryostat with the temperature set stable by a heater and a PID controller. The QDs were excited using the emission at 532 nm of a Nd:YAG laser focused on a spot with a diameter of about 80 μm. The PL signal was collected by a spherical mirror and sent into a 500 mm focal length spectrometer equipped with a 150 gr/mm grating and a Peltier-cooled CCD. The experimental results were then compared with numerical simulations based on an eight bands **k·p** model performed using the commercial software TiberCAD. Finally, the intraband spectrum was simulated based on the analysis of the PL results.

Results and discussion

In Figure 1(a)) are shown the PL spectra taken at 90 K of the selected sample for different values of the incident power. As can be seen, at the lowest power only the ground state transition of the QDs ensemble is visible. By increasing the excitation power, also the excited states become populated and therefore new transitions appear. The black dotted lines indicate the simulated transition energies of the ground state and of the first excited states. In the panel b of the same figure are reported the PL integrated intensities of the ground and the first excited state as a function of the excitation power. As can be seen, the intensity of the ground state emission increases linearly with increasing excitation power. On the other hand, the emission intensity of the first excited state increases more than linearly. This demonstrates that it is possible to control the population of each confined state in a precise way by changing the optical excitation power. In this work we are interested in the transitions involving the first two electron states at lower energies (i.e., ground state and first excited state). From the figure it is possible to see that 0.050 mW (corresponding approximately to 1 Wcm−2) is the highest power for which only the ground state is filled. On the other hand, 0.500 mW (corresponding approximately to 10 Wcm−2) is the largest power for which also the second state is populated, while the third state is still empty. Since the emission intensity is proportional to the filling of the states, by comparing the integrated intensities of the transitions it is possible to estimate the relative population density of the states at the selected powers and use it as an input parameter to simulate the intraband absorption spectrum.

We performed numerical simulations using an eight bands **k·p** model and envelope function approximation in

order to compute the transition energies and the optical matrix elements of those transitions. The simulated structure consists of a truncated cone QD made of GaAs with major and minor radius of 8 nm and 3.6 nm respectively[20] and a height of 8.2 nm, as obtained from the analysis of the AFM images, included in an Al0.3Ga0.7As barrier. The band-to-band transition between electrons and heavy holes states are indicated in Figure 1(a)) by dashed lines and show a good agreement with the experimental results. The calculated transition energies are 1.647 eV and 1.724 eV for the ground and the first excited state respectively. The computed optical matrix elements |M|2 for these transitions are 0.6414 a.u. and 0.0327 a.u. for the ground state and the first excited state transitions. The integrated intensity of a PL peak can be expressed as the product of a power-dependent effective carrier density and the optical matrix element:

$$I^{PL}_{GS(ES)}(P) = N^{eff}_{GS(ES)}(P)\left|M_{GS(ES)}\right|^2 \quad (1)$$

in which $I^{PL}_{GS(ES)}(P)$ is the PL integrated intensity shown in Figure 1(b)) of the ground (excited) state peak, $N^{eff}_{GS(ES)}(P)$ is the power-dependent effective carrier density of the ground (excited) state, and |MGS(ES)|2 are the optical matrix elements of the transitions. Therefore, by deconvoluting the PL spectra of Figure 1(a)) into its ground and excited state components, computing their integrated intensities (Figure 1(b)), and applying equation (1), it is possible to obtain the values of $N^{eff}_{GS(ES)}(P)$ at a chosen power. These values can then be used in the analysis of the IR photocurrent signal, in order to separate the contribution of the ground state and the first excited state transitions.

Based on the simulations, the obtained ground state and first excited state electron energies are at 0.212 eV and 0.138 eV below the Al0.3Ga0.7As barrier energy, corresponding to the transition wavelengths of 5.85 μm and 8.98 μm respectively. To simulate the absorption spectrum from the transition energies, we assumed the intraband absorption peak to have the same shape as the PL emission peaks (i.e., a Voigt function). For these transitions we considered the FWHM to be half of the one measured in the PL spectra (Figure 1(a)). This choice is based on the assumption that both electrons and holes states contribute to the broadening of the PL spectrum in a similar way. As a consequence, in first approximation we expect the FWHM to be halved for an intraband transition, where only the conduction band is involved. The intensity of the intraband absorption was then calculated using the effective carrier density obtained from equation (1) and assuming that the IR absorption is proportional to the filling of those states. Since the final state of the transitions that we are considering is a delocalized conduction band state (i.e., Bloch wave), we assume the optical matrix elements to be similar for both ground and first excited state. The resulting absorption spectrum is shown in Figure 2. In particular, in the case of

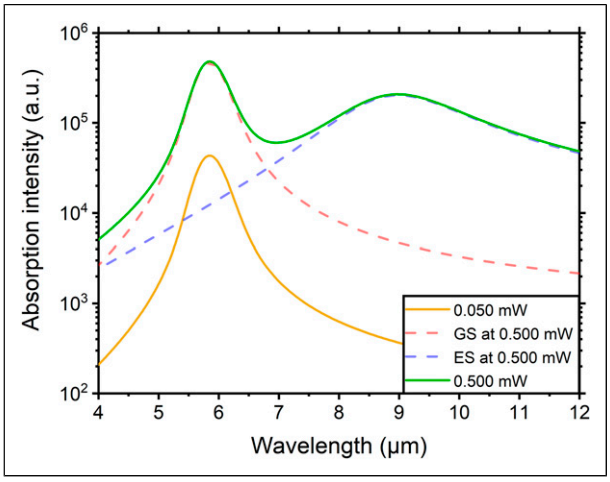

Figure 2. Simulated intraband absorption spectrum for ground and first excited state at a pumping power of 0.050 mW and 0.500 mW and a temperature of 90 K. The dashed lines show the simulated absorption spectra of the ground and the first excited state at a pumping power of 0.500 mW.

0.500 mW, the red and blue dashed lines show the contributions of the ground and the first excited state respectively.

As can be seen, for an exciting power of 0.050 mW a single absorption band peaking at 5.85 μm is expected, while for 0.500 mW a second band at 8.98 μm is present due to the filling of the first excited state. In the latter case, it is possible to note that the overlap between the two transitions is quite low. However, in an actual device being able to separate the contribution of the two transitions when measuring the photocurrent requires some initial calibrations. In the following, we will discuss a procedure to be able to determine the signal of each individual band.

Detection mechanism

In order to have a working detector that combines two absorption bands in the same structure, it must be possible to distinguish the origin of each signal. One possibility is to use a focal plane array with a grating that separates the spectral components of the incident light. However, this method cannot be used for a single pixel device. In this second case, the identification of the signal can be done by alternating the optical pumping power between 0.500 mW and 0.050 mW while continuously measuring the photocurrent. After an initial calibration, an unknown signal can then be decomposed into its components. This idea is based on the fact that the electron population inside the QDs is determined only by the pumping power, assuming the steady state behavior. This assumption is reasonable since, after a small transient, the system will be at the equilibrium as happens during PL measurements. Therefore, the signal can be deconvoluted into its components using a procedure

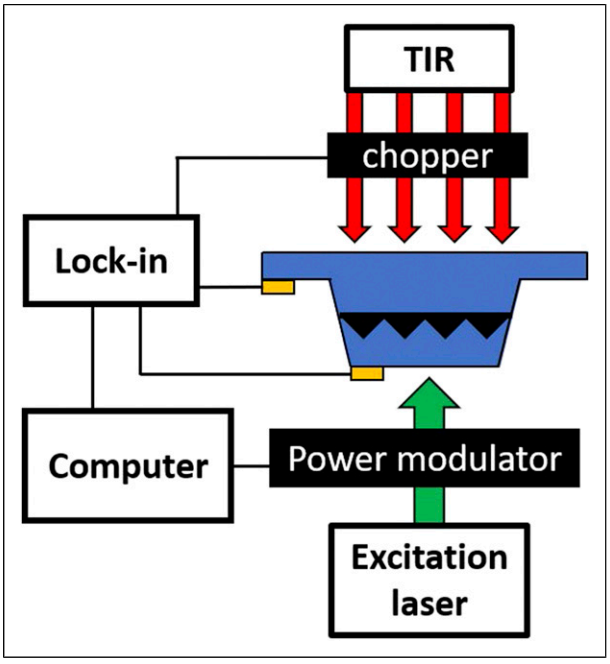

Figure 3. Schematics of the proposed device and its detection mechanism.

analogous to equation (1). Analyzing the PL spectrum gives information about the relative population of the states at the selected powers. Once this value is obtained, the photocurrent spectrum has to be measured by alternating the pumping powers in order to constantly change the QDs population density between the chosen values. At 0.050 mW the photocurrent is determined only by the absorption band peaking at 5.85 μm. When the excitation power is changed to 0.500 mW, the photocurrent originated from the ground state and the excited state transitions can be calculated by considering the new population densities of those states. It should be noted that the noise current can be affected by the carrier generation due to the optical pumping. Therefore, to take into account this aspect it is necessary to measure the noise current (i.e., current without IR light) for each pumping power. However, Ramiro et al. showed that in a similar device the noise current did not change significantly with the pumping power.[17] Figure 3 shows the schematics of the proposed device. The excitation laser reaches the sample from the top side of the mesa, so that the photogenerated carriers can reach and fill the QDs layer. A power modulator controlled by a computer continuously changes the incident excitation power between 0.050 mW and 0.500 mW in order to control the filling of the QDs states. The IR radiation incident from the bottom of the device is chopped and the photocurrent signal is then read by a lock-in amplifier and sent to the computer for the analysis. Thanks to the chopper and the power modulator, it is possible to distinguish the IR signal from the dark current in real-time at both excitation powers. Moreover, by performing a similar analysis to the one described above it is possible to separate the contribution of the two absorption bands.

Conclusions

In this work we have proposed a new idea for a dual-band infrared photodetector, the Optically Controlled Dual-band Infrared Photodetector (OCDIP). The working principle of this device is based on the possibility to dynamically change the QD states filling by varying the power of an optical pumping laser. Previous works used resonant excitation[16] or band-band optical transition17[15] to artificially dope the QDs ground state. The device proposed here takes these ideas and develops them in a way that controlling the pumping power allows to obtain one or two separate absorption peaks. We demonstrated the concept by growing a sample and measuring the PL spectrum at different operation powers of a visible laser. Based on the grown sample and the results of PL measurements, we simulated the intraband absorption spectrum at two selected power settings, namely 0.050 mW and 0.500 mW. The result shows the possibility to have one or two separated absorption bands which can be obtained by changing the optical pumping power. The possibility to have two absorption bands within the same structure and electronics may be an interesting solution for those applications where compact devices are required. One of the possible applications proposed in the manuscript is for remote monitoring of forest fires with drones, with the IR absorption bands covering a temperature range up to 200–300°C.

Acknowledgments

Francesco Basso Basset acknowledge financial support from the European Research Council (ERC) under the European Union's Horizon 2020 Research and Innovation Programme (SPQRel, Grant Agreement No. 679183) and by the European Union's Horizon 2020 Research and Innovation Program under Grant Agreement No. 899814 (Qurope)

Declaration of Conflicting Interests

The author(s) declared no potential conflicts of interest with respect to the research, authorship, and/or publication of this article.

Funding

The author(s) disclosed receipt of the following financial support for the research, authorship, and/or publication of this article: This work was supported by the ASI, Agenzia Spaziale Italiana (Grant no. DC-UOT-2018-024 - MUSICA - Multiband Ultrawide SpectroImager for Cryosphere Analysis) and by PIGNOLETTO project, co-financed with the resources POR FESR 2014-2020, European regional development fund with the contribution of resources from the European Union, Italy and the Lombardy Region.

ORCID iD

Stefano Vichi https://orcid.org/0000-0003-4272-4261

References

1. Hulley GC, Hook SJ, and Baldridge AM. Investigating the effects of soil moisture on thermal infrared land surface temperature and emissivity using satellite retrievals and laboratory measurements. *Remote Sens Environ* 2019; 114: 1480–1493.
2. Dozier JA. Methods for satellite identification of surface temperature field of subpixel resolution. *Remote Sens Environ* 1981; 11: 221–229.
3. Sobrino JA and Jiménez-Muñoz JC. Minimum configuration of thermal infrared bands for land surface temperature and emissivity estimation in the context of potential future missions. *Remote Sens Environ* 2014; 148: 158–167.
4. Jiang X, Li SS, and Tidrow MZ. Investigation of a multistack voltage-tunable four-color quantum-well infrared photodetector for mid- and long-wavelength infrared detection. *IEEE J Quan Electron* 1999; 35: 1685–1692.
5. Downs C and Vandervelde TE. Progress in infrared photodetectors since 2000. *Sensors* 2013; 13: 5054–5098.
6. Martyniuk P and Rogalski A. Quantum-dot infrared photodetectors: Status and outlook. *Prog Quan Electron* 2008; 32: 89–120.
7. Martyniuk P and Rogalski A. Insight into performance of quantum dot infrared photodetectors. *Bull Pol Acad Sci Tech Sci* 2009; 57: 103–116.
8. Sanguinetti S, Guzzi M, Grilli E, et al. Effective phonon bottleneck in the carrier thermalization of InAs/GaAs quantum dots. *Phys Rev B Condens Matter* 2008; 78: 1–6.
9. Rogalski A. Infrared detectors: An overview. *Infrared Phys Technol* 2002; 43: 187–210.
10. Martí A, Antolín E, Stanley CR, et al. Production of Photocurrent due to Intermediate-to-Conduction-Band Transitions: A Demonstration of a Key Operating Principle of the Intermediate-Band Solar Cell. *Phys Rev Lett* 2006; 97: 247701.
11. Scaccabarozzi A, Adorno S, Bietti S, et al. Evidence of two-photon absorption in strain-free quantum dot GaAs/AlGaAs solar cells. *Phys Status Solidi RRL* 2013; 7: 173–176.
12. Pan D, Towe E, and Kennerly S. Normal-incidence intersubband (In, Ga)As/GaAs quantum dot infrared photodetectors. *Appl Phys Lett* 1998; 73: 1937–1939.
13. Liu HC. Quantum dot infrared photodetector. *Opto-electron Rev* 2003; 11: 1–5.
14. Yakimov AI, Timofeev VA, Bloshkin AA, et al. Influence of delta-doping on the performance of Ge/Si quantum-dot mid-infrared photodetectors. *J Appl Phys* 2012; 112: 034511.
15. Attaluri RS, Annamalai S, Posani KT, et al. Influence of Si doping on the performance of quantum dots-in-well photodetectors. *J Vac Sci Technol B* 2006; 24: 1553–1555.
16. Höglund L, Holtz PO, Pettersson H, et al. Optical pumping as artificial doping in quantum dots-in-a-well infrared photodetectors. *Appl Phys Lett* 2009; 94: 053503.
17. Ramiro I, Martí A, Antolín E, et al. Optically triggered infrared photodetector. *Nano Lett* 2015; 15: 224–228.
18. Watanabe K, Koguchi N, and Gotoh Y. Fabrication of GaAs quantum dots by modified droplet epitaxy. *Jpn J Appl Phys* 2000; 39: 79–81.
19. Gurioli M, Wang Z, Rastelli A, et al. Droplet epitaxy of semiconductor nanostructures for quantum photonic devices. *Nat Mater* 2019; 8: 799–810.
20. Bietti S, Bocquel J, Adorno S, et al. Precise shape engineering of epitaxial quantum dots by growth kinetics. *Phys Rev B* 2015; 18: 075425.
21. Basso Basset F, Bietti S, Tuktamyshev A, et al. Spectral broadening in self-assembled GaAs quantum dots with narrow size distribution. *J Appl Phys* 2019; 126: 024301.
22. Vichi S, Bietti S, Khalili A, et al. Droplet epitaxy quantum dots based infrared photodetectors. *Nanotechnology* 2020; 31: 245203.
23. Tuktamyshev A, Fedorov A, Bietti S, et al. Nucleation of Ga droplets self-assembly on GaAs(111)A substrates. *Sci Rep* 2021; 11: 6833.
24. Jo M, Mano T, and Sakoda K. Unstrained GaAs Quantum Dashes Grown on GaAs(001) Substrates by Droplet Epitaxy. *Appl Phys Express* 2010; 3: 045502.
25. Sanguinetti S, Mano T, Gerosa A, et al. Rapid thermal annealing effects on selfassembled quantum dot and quantum ring structures. *J Appl Phys* 2008; 104: 113519.